Comparison of giant multipole resonances of multipolarity $E1$ to $E4$ in ^{58}Ni ($T_0 = 1$) and ^{60}Ni ($T_0 = 2$) with inelastic electron scattering

R. Pitthan,* G. M. Bates, J. S. Beachy, E. B. Dally,† D. H. Dubois, J. N. Dyer, S. J. Kowalick, and F. R. Buskirk
Department of Physics and Chemistry, Naval Postgraduate School, Monterey, California 93940
(Received 3 April 1979)

The cross section for electron scattering from the isotopes ^{58}Ni and ^{60}Ni has been measured with electrons of 102 MeV at scattering angles of 45, 60, 75, 90, and 105° between 3 and 50 MeV excitation energy. Resonances or resonancelike structures at approximate excitation energies of (7–8) MeV, 13 MeV, (16–17) MeV, (18–19) MeV, 27 MeV, 32 MeV, and 40 MeV were classified on the basis of their momentum transfer dependence and discussed in the framework of the shell model. Difficulties in the extraction of the cross section and model dependencies of the interpretation are discussed.

[NUCLEAR REACTIONS ^{58}Ni (e,e') and ^{60}Ni (e,e'), $E_0 = 102$ MeV. Measured $d^2\sigma/d\Omega dE_x$, bound and continuum states (giant resonances). Deduced multipolarity, reduced matrix element $B(E\lambda)$, sum rule exhaustion of giant resonances, total width of continuum and clustered states.]

I. INTRODUCTION

The conservation of isospin in electromagnetic nuclear interactions has as a consequence that in non-self-conjugate nuclei ($N \neq Z$, ground state isospin $T_0 \neq 0$) the giant dipole resonance, in fact any isovector state, has two components with $T_< = T_0$ and $T_> = T_0 + 1$ (Ref. 1). Since the splitting is found to be several MeV, it can be observed experimentally.[2] Moreover, the predicted strength B of the two components is comparable for small T_0. Observation of isospin splitting should, therefore, be especially easy and convincing for the two target nuclei of this investigation.

According to the isospin selection rules an excited state with isospin T_0 can decay by both proton and neutron emission into low-lying states of the daughter nuclei with $T_0 \pm \frac{1}{2}$, but a state with $T_> = T_0 + 1$ can only decay by proton emission, since in the case of neutron emission the isospin to be transferred would have to be $\frac{3}{2}$. Since proton emission from the lower state $T_<$ will be more inhibited by the Coulomb barrier than that from the $T_>$ state, it has been argued that the $T_<$ states will decay preferentially by neutron decay and the $T_>$ states by proton decay. The experimental finding in photonuclear experiments that the ratio of proton to neutron strength is approximately 2:1 in ^{58}Ni, but 1:2 in ^{60}Ni (Refs. 3 and 4) has been interpreted as evidence for isospin splitting.[4] Later γ work cautions in respect to this interpretation.[5]

Although single arm (e, e') experiments do not measure the decay channels, we thought it interesting to measure the total strength function for this pair of $T = 1$ and $T = 2$ nuclei under the aspect of isospin for several reasons: (1) The total $E1$ cross section has not yet been measured. It is important to check whether or not the particle channels, mainly (γ,n), (γ,p), and (γ,pn) add up to the total cross section. (2) As already mentioned, any isovector state could show isospin splitting.[6] Since in recent years evidence for an isovector quadrupole resonance has been found in many nuclei with $A \gtrsim 89$ (see Fig. 1 in Ref. 7) we wanted to locate this strength in the Ni isotopes and investigate possible splitting or shifts of strength. (3) There are other continuum states in ^{58}Ni and ^{60}Ni which have been assigned contradictory multipolarities. They also could be subject to isospin dependent interactions.

From the experience in other nuclei it might be stated that excitation energy and strength of $E1$, $E2$, and $E3$ resonances vary only slowly as a function of A. Differences in gross structure have primarily been reported for the giant dipole resonance (GDR)[8] and low-lying $E3$ states at $\sim 30\,A^{-1/3}$ MeV (Ref. 9) between spherical and deformed nuclei. Since both Ni isotopes investigated here have spherical ground states and very similar level schemes for the lowest levels, large differences between ^{58}Ni and ^{60}Ni, therefore, naively would have to be primarily interpreted in terms of isospin effects.

II. EXPERIMENTAL DETAILS

The experiments discussed in this paper used electrons of primary energy of 102 MeV from the three section, S band, linear accelerator of the Naval Postgraduate School.[10] The scattering angles were 45, 60, 75, 90, and 105°, corresponding

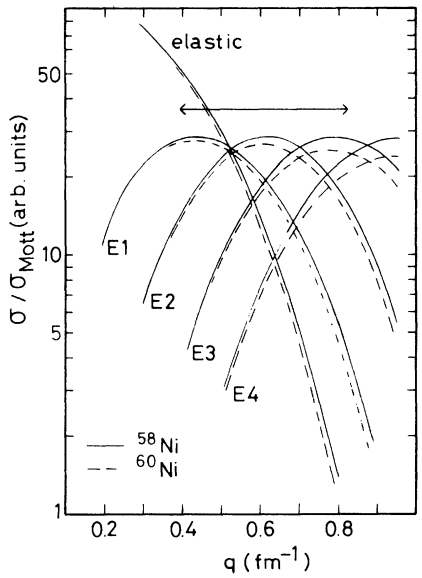

FIG. 1. Comparison of DWBA cross sections divided by the Mott point nucleus cross section (form factors) for inelastic $E1$ to $E4$ transitions and elastic scattering. The arrow indicates the momentum transfer covered. The curves are calculations for a primary energy of 102 MeV and are normalized so that the first maxima are equal. Although for a nucleus with a finite charge they no longer correspond to pure Bessel functions in the radial integral, the Bessel function pattern is still visible. Note especially that the elastic cross section does not fall off with lower momentum transfer, but instead rises, making low momentum transfer measurements very difficult. For the $E2$, $E3$, and $E4$ transition the Goldhaber-Teller (Tassie) model was used; the $E1$ was calculated with the Myers-Swiatecki model as described in the text.

to an elastic momentum transfer from 0.40 to 0.82 fm^{-1}. As Fig. 1 shows, this range is large enough to distinguish between multipolarities $E1$ to $E4$. The elastic relative cross section is also indicated in Fig. 1; it does not vanish at low momentum transfer. The targets were self-supporting with thicknesses between 35 and 140 mg/cm^2, depending on the scattering angle; they were enriched to better than 98% in the respective isotope. The inelastic spectra were measured relative to the elastic cross section.

Before scattering, the electrons are momentum analyzed in the symmetry plane of a two 30° sector magnet achromatic deflection system.[10] After scattering, the electrons are measured by a 10 counter ladder in the focal plane of a 40 cm, 120° double focusing spectrometer with a momentum bite of 3%.

The resolution, defined by a slit system between the deflection magnets, was kept at 0.5%, because this was the setting found to produce the least background.

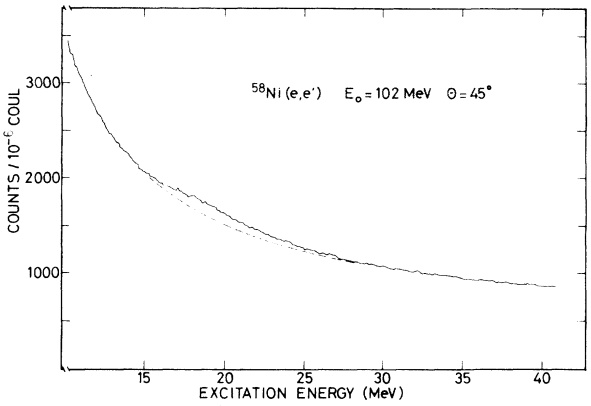

FIG. 2. Spectrum of 102 MeV electrons scattered inelastically from ^{58}Ni at 45° in the giant resonance region. Note that the zero for the count rate is *not* suppressed. The resonant cross section, which consists to 80% of $E1$, is clearly visible above the smooth background. Even at this angle, where the signal to background ratio is the smallest of all spectra taken, the resonant cross section corresponds to 8% of the total count rate. The accuracy in the extraction of the $E1$ cross section is comparable to that of larger angles (higher momentum transfer), because of 45% the uncertainty arising from higher multipolarities is small.

The stepping width of the spectrometer magnetic field normally corresponds to 0.1 MeV; the 10 spectra of the individual counters of the counter ladder are energy sorted into 0.1 MeV energy bins. For control purposes, the whole excitation range was scanned with a 2 MeV stepping width before and after each inelastic run. No deviations were found except for the 60° spectrum of ^{60}Ni in the 25 to 30 MeV region.

Typical spectra are shown in Figs. 2 and 3. These figures, together with Fig. 1, illuminate the problem of low momentum transfer experiments. Since the radiation tail is, in first order, proportional to the elastic cross section, it dominates the 45° measurements, where it constitutes more than 90% of the total cross section, whereas the radiation tail is only of the same order of magnitude as the resonant cross section at 105°. At the larger angle, however, higher multipoles contribute, making the disentangling of the resonances more difficult.

III. EVALUATION

Figure 2 showed a spectrum for ^{58}Ni as measured by the magnetic spectrometer. It demonstrates one of the main difficulties to be overcome: At low momentum transfer the resonant cross section, mostly $E1$ as we will show below, is only a small fraction of the total cross section, which is composed mainly of the radiation tail. This

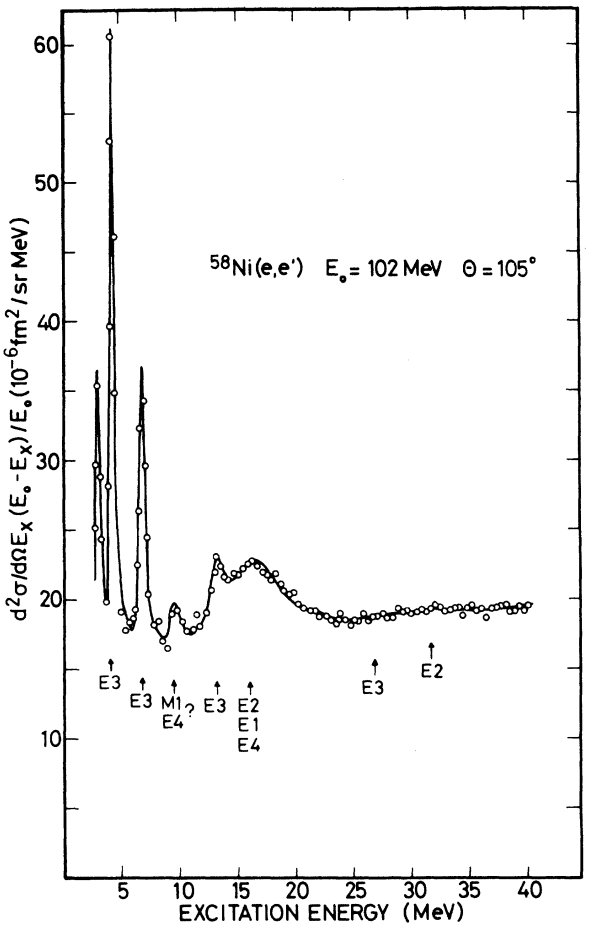

FIG. 3. Spectrum of 102 MeV electrons scattered inelastically from ^{58}Ni at 105°. The spectrum clearly shows the transition from the sharp bound states to the broad continuum states. Note that the zero is not suppressed; the giant resonance cross section is a sizable fraction of the total cross section including the radiative and experimental background. The cross section has not been corrected for the constant magnetic dispersion of the spectrometer. For graphical purposes, the number of points shown (measured were 10 points/MeV) has been reduced by a factor of 2 below 10 MeV, and by a factor of 4 above. The arrows indicate the assignments made in this work. The statistical error is of the size of the circles representing the data; the overall resolution was 500 keV.

situation occurs because the radiation tail rises approximately in inverse proportion to q^4 (Mott cross section), while, for small momentum transfer, the $E1$ cross section varies only slowly. Improvements on the radiation tail calculation have been reported recently.[7] The main point is the use of the exact elastic cross section, calculated with the program of Fischer and Rawitscher,[11] in the (Born approximation) formalism of Ginsberg and Pratt[12] and the use of exponentiation in Schwinger and bremsstrahlung corrections to the elastic peak to account for multipole photon emission and finite target thickness effects,[7] respectively.

For the radiation tail in the immediate vicinity of the elastic peak, it is of no importance which elastic cross section one takes, because the calculation can always be normalized to the measured area under the elastic peak, i.e., the cross section. However, in some of the contributions to the radiation tail the cross section of the outgoing electron enters and it is of prime importance that the ratio of $\sigma(E_i)/\sigma(E_f)$ is correct for large differences between E_i and E_f, which is only the case if one uses phase shift calculated cross sections. Most electron scattering groups now use this method with excellent results.[13,14] The main theoretical question remains: Why is this apparently *ad hoc* improvement so successful?

As described elsewhere,[7] the total background BGR (including the radiation tail) in our measurements can be described by an equation with two free parameters: $\mathrm{BGR}(E_f) = P_1 + P_2/E_f + \mathrm{TR}$ (for details see Ref. 7). This is an important reduction in the number of free parameters needed because a polynomial fit to the background without using the calculated radiation tail would have to use 7–9 parameters. The point we are trying to make is that the simple form of BGR reduces the arbitrariness in the background definition compared to an *ad hoc* polynomial fit.

Our confidence in the method of evaluation is enhanced by the agreement of our results in heavy nuclei with (γ, n) (for the $E1$ resonance) and (α, α') (for the $E2$ resonance). Another test is less involved but more instructive. Using a french curve and trying to fit a monotonic background (the radiation tail is known to be a monotonic function of E_x) into Fig. 2 it is very difficult to come up with a curve different from the one shown if one uses as a boundary condition that the radiation tail has to smoothly connect with the measured cross section below 15 and above 30 MeV, where no noticeable cross section is expected at this low momentum transfer. In any case, the radiation tails for ^{58}Ni and ^{60}Ni will be essentially the same except for effects due to minor differences in the ground state charge distributions.

However, we would like to emphasize that a careful quantitative investigation is always in order. A difference in the ground state R_{ms} value between the two isotopes of less than 2% amounts to a difference in the elastic cross sections which rises from 4% at 45° to 20% at 105° (Fig. 1). This situation arises because our measurements take place close to the first minimum in the elastic form factor, which for $Z = 28$ is not yet filled in

as in heavy nuclei. Therefore, for all elastic and inelastic calculations separate c, t values for the ground state charge distribution of the two isotopes were used. These values were taken from the compilation of the de Jager *et al.*, and were $c = 4.098$ fm and $t = 2.454$ fm for ^{58}Ni and 4.147 fm and 2.522 fm for ^{60}Ni.

The radial momenta needed for calculating the sum rules[10] connected with these parameters are $\langle r^2 \rangle = 14.37$ fm^2, $\langle r^4 \rangle = 253.5$ fm^4, and $\langle r^6 \rangle = 4753$ fm^6 for ^{58}Ni, and 14.86 fm^2, 270.2 fm^4, and 5212 fm^6, respectively, for ^{60}Ni.

Even more than in heavier nuclei, it was found that the real problem in disentangling the spectra did not consist in the subtraction of the radiation tail, but rested in the overlap of the resonances. It is known that the $E1$ resonance energy in nuclei falls off faster than predicted by an $80\,A^{-1/3}$ law[8] while the $E2$ resonance stays fairly constant at $63\,A^{-1/3}$ MeV [15] In the Ni region the $E1$ ($\Delta T = 1$) and $E2$ ($\Delta T = 0$) giant resonances are thus not separated widely enough to necessarily allow a clear determination of the line shape at medium momentum transfer ($q \gtrsim 0.5$ fm^{-1}), where the two cross sections are of comparable magnitude.

To overcome this problem the measurements were extended to low momentum transfer. Figure 1 shows that below 0.5 fm^{-1} the $E1$ cross section is dominant while the $E2$ dominates above 0.7 fm^{-1}. From this measurement the $E1$ line shape was determined in both nuclei, found to be sufficiently different from $E2$, and used for a line shape fit of the middle points. The (γ, n) data for ^{58}Ni and (γ, p) data for both isosopes do not support the treatment of the giant resonance region with simple Breit-Wigner curves. However, our spectra could be fitted with the expected theoretical χ^2 value (for details see Refs. 10 and 16), thus indicating that the total cross section is not as structured as the sum of the partial channels indicates. In addition, one does not have to attach a deeper meaning to the use of line shapes, and should regard them rather as model-independent vehicles to extract the areas under the measured differential cross section.

Since the electron is an electromagnetic probe, the transition strength distribution underlying the resonant cross section can be determined in a nearly model-independent way by a line shape fit. To maximize the accuracy of the extraction of the multipolarity and to enable investigation of the model dependency of the stronger resonances, which requires small relative errors (relative from angle to angle), our final fits used, as justified in more detail below, the same constant average line width for all angles measured. This can be done because the form of the electromagnetic strength distribution (B value) is independent of electron energy and angle.

It is obvious from the complexity of the spectra, with so many broad overlapping resonances, that a totally unconstrained fit with three fit parameters per resonance (for position, height, and width) is nearly impossible.

The procedure for our attempts to unravel the spectra then can be described as follows: The position of a resonance is determined most easily and accurately, followed by the width, which for the high-lying resonances, however, may be very difficult to estimate. In the final fits, examples

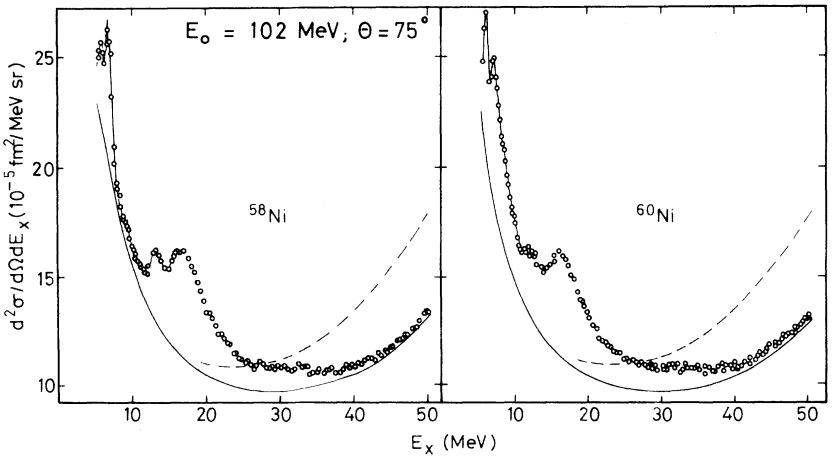

FIG. 4. Comparison of spectra of 102 MeV electrons scattered at 75° from ^{58}Ni and ^{60}Ni. The cross section for ^{60}Ni has been renormalized so that the highest and lowest points in both plots are equal. The spectra were taken with 10 points/MeV but have been reduced for graphical purposes. The broken line is the calculated radiation tail. For demonstration purposes we have subtracted the ghost peak at 8 MeV from the data for ^{58}Ni, but not for ^{60}Ni; the difference is clearly visible. Note the suppressed zero.

of which are shown in Figs. 4–7, we would usually keep position and width to the average value of previous fits. The statistical error for the area under the resonance is determined by the error in height and width. Since we keep the width constant, the error will be unrealistically small. It is, therefore, not possible to use the error from the evaluation of the error matrix of the final fit for the overall uncertainty assignment of the transition strength. We rather use the minimum and maximum values for the resonance areas found during the many trial computer fits performed (usually 50 to 100 per spectrum).

However, for the determination of multipolarities, the situation is different. Since we keep the width constant to the average value, a deviation from the true (also constant) value will influence the strength of this resonance in all spec-

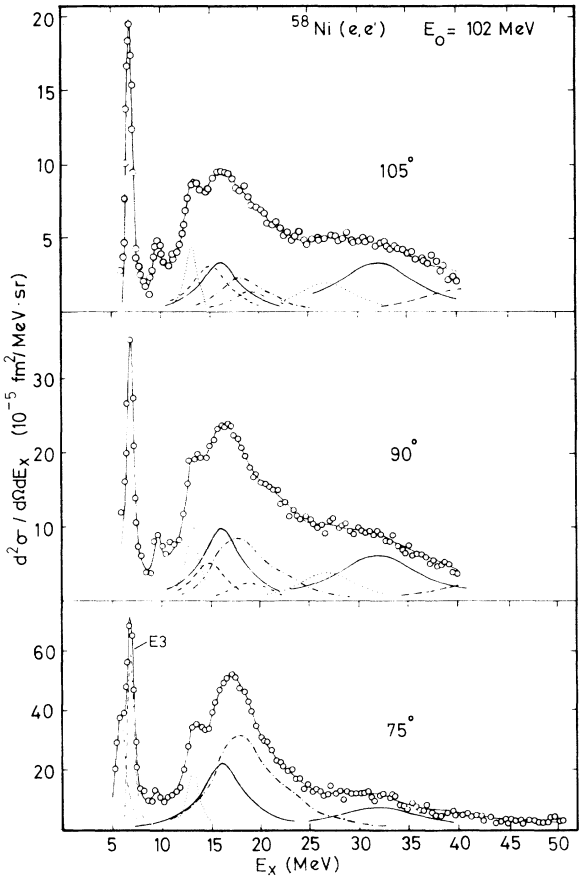

FIG. 5. Comparison of inelastic electron spectra for ^{58}Ni scattered at 75, 90, and 105°. The typical feature of higher multipolarities ($E3$ and $E4$) becoming more pronounced as compared to $E1$ and $E2$ with higher momentum transfer are most clearly visible for the $E3$ states at 7 and 13 MeV. The solid lines represent $E2$, the dotted lines $E3$, the broken lines $E4$, and the broken-dotted ones $E1$. For more details concerning assumptions about multipolarities and their possible interplay the text should be consulted. The tail of the resonance at 40 MeV (broken line) for 90 and 105° has been taken from the ^{60}Ni measurements (Fig. 6) because the ^{58}Ni data extended only to about 40 MeV.

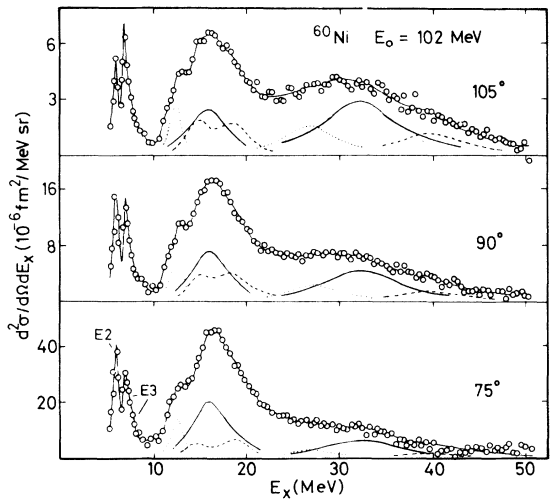

FIG. 6. Similar to Fig. 5, but for ^{60}Ni. The $E1$ has been omitted and the $E4$'s at 15 and 19 MeV have been added into one line for clarity (but see remark in Sec. IV F).

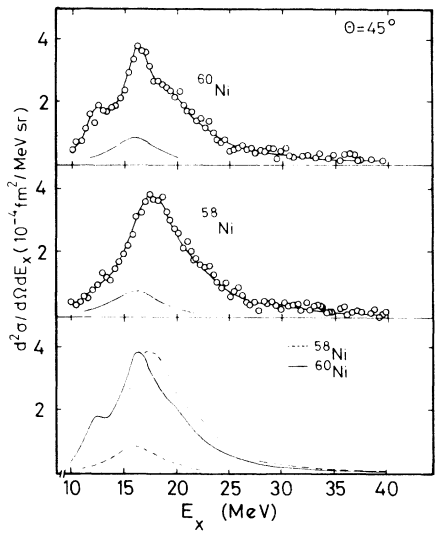

FIG. 7. (a) Data of Fig. 2 after subtraction of radiative background, experimental background, and $E2$ and $E3$ resonances known from measurements at higher momentum transfer. For graphical purposes, the number of data points has been reduced by a factor of 4. (b) Same as Fig. 3(a), but for ^{60}Ni. (c) The fitted curves of parts (a) and (b), in comparison. A downward shift of the maximum of approximately 1.3 MeV is visible; 0.25 MeV of this would be due to the simple $A^{-1/3}$ MeV rule, the remainder is in qualitative agreement with the isospin coupling model. Agreement of the details of the change in strength distribution is not so good (see text).

tra similarly; that means it will have the same effect as a systematic error. This difference in the uncertainty of the strength and the multipolarity leads to the situation where, in many papers, apparently too large an error is assigned for the sum rule exhaustion, at least if one deduces the total error from the relative errors of the angular or momentum transfer distribution alone.

It would not be possible to make a meaningful decomposition of the continuum cross section with just one spectrum, with, as in the present case, the possible exception of the 45° and the $E1$ resonance. An additional condition has, therefore, to be fulfilled—the consistency of the fits to the various angles. What does "consistency" mean here?

"Consistent" fits in other nuclei, where the resonances of different multipolarity are far enough apart for separation by a line shape fit, means consistent results for excitation energy and width. In the Ni isotopes the $E1$ and $E2$ resonances around 16 MeV are so intertwined that a further consistency condition had to be imposed as a fitting constraint, namely, the resonances had to follow the form factor associated with $E1$ and $E2$. The following procedure was employed. $E1$ strength was determined using the 45° and 60° spectra, where contributions from higher multipolarities are small and can be safely estimated from backward angles, and where, in addition, position and width of the $E2$ may be taken from (α, α'),[17] information which is reliable and relatively model independent. Unlike the situation for heavier nuclei, no equally reliable information is available in Ni isotopes for the $E1$ strength from photon experiments because, as mentioned before, it is *not* identical with the (γ, n) cross section. Four resonances each were found necessary to describe the $E1$ cross section. In the next step the isoscalar $E2$ strength was kept constant to values of 45, 50, 55, 60, and 70% of the sum rule using the Goldhaber-Teller model (see below), while fitting the $E1$ (and the other resonances) at all angles. These fits produced consistent results for the $E1$ only for certain values of the $E2$ strength, if the $E1$ strength was a free fitting parameter at all angles. Consistent for the $E1$ means that it followed the Myers-Swiatecki (MS) form factor (see below).

In turn then, the $E1$ strength was kept constant to the average strength from the MS model (Table II), and the isoscalar $E2$ (and other resonances required to describe the total differential cross section) were fit freely. Using this method in an iterative procedure, values for $E1$ and $E2$ strength were established. While doing so, we found that we had to change the parameters for position and width of the $E2$ resonance slightly from the initial values taken from (α, α'),[17] to achieve consistency at all angles measured.

One shortcoming should be emphasized. The procedure just described is based on the assumption of a certain form factor, similarly, but not quite as heavily, model dependent as a multipole expansion.[14] The form factors in our case were based on the Goldhaber-Teller (Tassie) model for the $E2$ and the Myers-Swiatecki model for the $E1$. This introduces a model dependence, however reasonable this assumption may be. If one wants to look more positively at the situation, one might in turn claim that the consistency established constitutes a verification of the models used. This might be regarded a valid argument especially for the $E1$, where the model sensitivity is very large, much larger than in heavy nuclei. Similar to the case of the elastic cross section described above, the minima in the form factors are not filled in as much as in heavy nuclei. It is apparent from Fig. 8 that consistency in the above described situation for the $E1$ and $E2$ at 16 MeV will most likely only be possible with one of the $E1$ models considered, which in fact, turned out to be the Myers-Swiatecki model (Fig. 9). It should be reemphasized at this point that these difficulties are less due to uncertainties in the background subtraction, rather they rest in the existence of overlapping resonances.

Only one other spectral region caused major problems in the evaluation. As Fig. 5 shows, the data at 90° and 105° for ^{58}Ni only go to 40 MeV

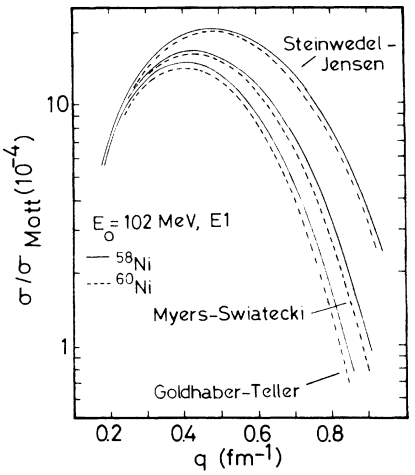

FIG. 8. Comparison of $E1$ DWBA calculation based on the three models indicated. The curves are normalized to $B(E\lambda) = 1$ fm^2. It is evident that the experimentally extracted strength will depend on the model used. Measurements in other nuclei indicate that the Myers-Swiatecki model describes the data best. To a limited extent this is also borne out by this experiment (see Fig. 9 and text).

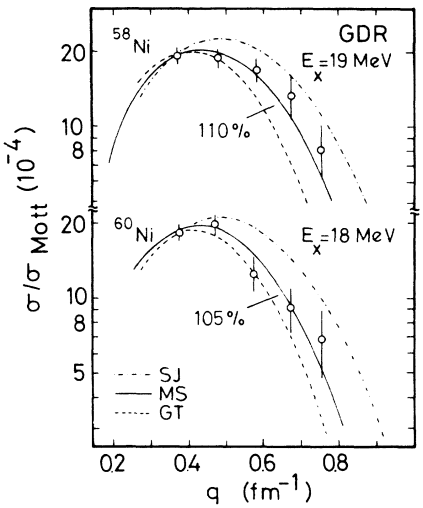

FIG. 9. Comparison between experimental and calculated cross sections for the models of Fig. 8. The curves were normalized to go through the point with the lowest momentum transfer, because this is the one with the least model dependence and the most accurate one. The Myers-Swiatecki model is somewhat favored by this comparison; however, the difficulties with the simultaneous fit of several resonances between 15 and 19 MeV, as discussed in the text, should be noted.

excitation energy. Since we found a resonance at 40 MeV in ^{60}Ni, we assumed a resonance with the same strength in ^{58}Ni, which had to be kept to a constant value.

It has been pointed out in the foregoing that owing to the constraints which had to be put on $E2$ and $E1$ cross sections a model dependence is introduced. How large is this model dependence?

Traditionally two models have been used to describe the GDR. The model which regards the dipole mode as an oscillation of interpenetrating proton and neutron liquids within a fixed boundary, first described by Migdal,[18] has been independently proposed by Goldhaber and Teller[19] and treated in detail and greatly expanded by Steinwedel and Jensen.[20] Not quite logically it is generally referred to as the Steinwedel-Jensen model. The transition charge density derived from this model is

$$\rho_{\rm tr}^{\rm SJ}(r) = C_{\rm SJ}\, j_1(r\,2.08/c)\rho_0(r)$$

(c is the half density radius, j_1 the spherical Bessel functions of first order). The ground state charge distribution $\rho_0(r)$ is not included in the original treatment, but relaxes the unphysical condition of a rigid surface. The above form for $\rho_{\rm tr}^{\rm SJ}(r)$ leads to only minimal deviations in the calculated cross section compared to the form we used recently.[10] The Goldhaber-Teller model (model 3 of Ref. 19) leads to a transition charge density

$$\rho_{\rm tr}^{\rm GT}(r) = C_{\rm GT}\, r^{\lambda-1} d\rho_0(r)/dr\,,$$

identical to that of the Tassie model.[21]

How much is this model dependence for Ni at the lowest momentum transfer $q = 0.37$ fm^{-1}? In plane-wave Born approximation (PWBA) the form factor is defined by

$$F^2(q) = 4\pi/Z^2(2\lambda+1)\left|\int j_\lambda(qr)\rho_{\rm tr}(r)dr\right|^2 .$$

By developing the Bessel function and discarding constants one gets

$$F^2(q) \propto |[1 - \tfrac{1}{10}q^2\langle r^2\rangle_{\rm tr}]|^2$$

for a dipole transition. The q^4 term, with a coefficient of $\frac{1}{280}$, may be neglected. For photon experiments with $q = k = E_x/\hbar c$ the second term in the bracket is less than 0.025 for Ni with $E_x \approx 20$ MeV and $\langle r^2\rangle_{\rm tr} < 25$ fm^2. In the case of the present experiment with $q = 0.37$ fm^{-1} the second term is 0.24 for the SJ model, with $\langle r^2\rangle_{\rm tr} = 17.5$ fm^2, and 0.34 for the GT model, with $\langle r^2\rangle_{\rm tr} = 24.5$ fm^2. The resulting ratio in the square of the form factor with DWBA calculations is 0.79, i.e., if the extracted strength with the SJ model is 100%, the GT strength would be 127% energy-weighted sum rule (EWSR). In heavy nuclei and for higher momentum transfer the ratio of the cross sections predicted by SJ and GT models has been found to be roughly 1 : 2, in some cases clearly ruling out the SJ model.

Conventionally (e, e') measures $B(E\lambda, q = 0)$ which is connected with $B(E\lambda, q = k)$ extracted from photon experiments by the expression which was derived above for the model dependency, because the B value is defined by

$$B(E\lambda) = (2\lambda+1)\left|\int j_\lambda(kr)\rho_{\rm tr}(r) r^2 dr\right|^2 .$$

Thus, before the two values can be compared, the (γ, n) value has to be corrected to $q = 0$. The correction is typically 5% and changes very little with A because the excitation energy of the giant dipole resonance varies with $A^{-1/3}$, but the radius varies with $A^{+1/3}$.

Recently Myers *et al.*, on the basis of Myers' and Swiatecki's droplet model,[22] have shown that the transition density should be a mixture of both SJ and GT models.[23] Figure 8 shows the resulting form factor if we use their transition density for Ni, namely

$$\rho_{\rm tr}^{\rm MS}(r) = C_{\rm MS}[\rho_{\rm tr}^{\rm GT}(r) + 0.55\rho_{\rm tr}^{\rm SJ}(r)]\,,$$

in the DWBA calculations. Using $\rho_{\rm tr}^{\rm MS}$ instead of $\rho_{\rm tr}^{\rm GT}$ reduces the resulting transition strength by 7% for 45°. That the real transition density should be some combination of SJ and GT models may also be inferred from the A dependence of the

resonance energy. The GT model predicts the excitation energy of the GDR to vary like $A^{-1/6}$, the SJ predicts $A^{-1/3}$, while the experimental energies[8] are well described by $A^{-0.23}$. The amount of admixture of the SJ to the GT model found by Myers *et al.*[23] rises from 50% to 80% for nuclei between Ni and ^{208}Pb. The average value is in quantitative agreement with an $A^{-0.23}$ rule.

In summary then, one might state the following for the evaluation of the experiments described here: (1) The radiation tail is high, but it can be handled well enough to allow an extraction of the resonant part of the total cross section. Because the treatment and subtraction of the radiation tail in the past has been a major criticism concerning (e, e') excitation of the continuum, we would like to emphasize that the low excitation energy part, where the true radiation tail is known from experiment between isolated levels, is reproduced, and that our total background approaches the high excitation energy part ($E_x > 40$ MeV), where only a marginal cross section is expected, asymptotically. (2) Due to the variation of momentum transfer available the $E1$ and $E2$ GR can be disentangled. (3) The need to use a model for the transition charge density in the DWBA calculations introduces a model dependence into the B values, but not the cross sections, because of the use of the line shape fit. However, reasonable assumptions about the model used show that the $E1$ B values are lower by 7–12% between 45 and 75° in both nuclei if one uses the Myers-Swiatecki model instead of the Goldhaber-Teller model. Throughout this paper numerical results for the $E1$ are based on the use of the MS model.

A difficulty common to all single arm scattering experiments exciting giant resonances is the assignment of a proper error. The problem arises from the uncertainty in the determination of the underlying nuclear continuum in the case of hadron scattering, and the radiative continuum in the case of (e, e'). Errors assigned to the experimental cross sections are mostly determined from the variations produced by varying the background within reasonable limits.

The errors given below are estimated errors based on this method; they are roughly two times the statistical errors. Possible systematic uncertainties from the use of a certain model have been discussed. Other systematic errors like target thickness, solid angle, counter efficiencies, absolute charge integration, etc., cancel because the inelastic cross sections are determined relative to the elastic ones, which, in turn, are calculated from tabulated experimental ground state charge distributions. The total uncertainty in the elastic reference cross section may safely be estimated to be smaller by 3%. For the special case of the $E1$ strength, additional uncertainty from underlying higher multipolarities should also be negligible.

IV. RESULTS

A. General

The widely accepted framework for a general look at giant resonances (GR's) (the nuclear continuum above approximately the particle thresholds and below the quasielastic region) is the Bohr-Mottelson self-consistent shell model.[24] If we follow the schematic random-phase approximation (RPA) calculations based on this model,[25] the structure of the giant resonance region evolves as follows. Without isospin a GR would be at the energy corresponding to main shell transitions ($\hbar\omega_0 = 41\, A^{-1/3}$ MeV) allowed by spin and parity, e.g., $1\hbar\omega_0$ and $3\hbar\omega_0$ for an $E3$ excitation. The effect of the isospin on the particle hole interaction splits these transitions into isoscalar and isovector ones, because the residual ph force is

TABLE I. Random phase approximation (RPA) calculations of Hamamoto (Ref. 25) for the principal main shell transitions into the continuum. While this simple model naturally cannot account for finer details, such as the fine structure found in ^{208}Pb, it describes the overall picture quite well.

Multipolarity λ	Unperturbed energy units of $\hbar\omega_0$ [a]	Isoscalar modes E_x ($A^{-1/3}$MeV)	Isoscalar modes R [a]	Isovector modes E_x ($A^{-1/3}$MeV)	Isovector modes R [b]
2	2	58	100	135	100
3	1	25	28	53	2
	3	107	72	197	98
4	2	62	51	107	3
	4	152	49	275	97

[a] $\hbar\omega_0 = 41\, A^{-1/3}$MeV.
[b] $R = E_x B(E\lambda, q=0)/\mathrm{EWSR}(E\lambda, T)100$.

attractive for isoscalar modes and repulsive for isovector modes.

Table I shows results from Ref. 25 for $E2$, $E3$, and $E4$ transitions. It should be pointed out that according to these calculations the isovector strength is nearly totally concentrated into the mode higher in excitation energy, e.g., $4\hbar\omega_0$ in the case of a hexadecupole GR. Of course, one should not expect that the actual behavior of the nuclei is totally determined by this simple picture, especially since the low-lying isoscalar $E3$ has been found to be more complicated, but the general agreement is very good and the Bohr-Mottelson description has generally been used as a classification scheme.

Figure 1 showed the inelastic form factors as a function of momentum transfer. Although the plane-wave Born approximation is no longer strictly valid, the figure still shows the typical Bessel function pattern. If one, e.g., picks out the $E2$ cross section, it is evident that an $E1$ transition would appear to rise slower with momentum transfer whereas an $E3$ would rise faster. If one knows which part of the cross section in an inelastic spectrum is $E2$, some qualitative results are immediately apparent.

Figures 5 and 6 show the spectra of 102 MeV electrons scattered inelastically from ^{58}Ni and ^{60}Ni, respectively, at 75°, 90°, and 105°. The solid curves in both figures represent the isoscalar and isovector giant quadrupole resonance at 16 and 32 MeV. Several distinct features are visible without detailed analysis. The state at 17 MeV is very peaked in ^{58}Ni, more fragmented in ^{60}Ni, but rises faster than $E2$ in both. A state around 9.5 MeV in ^{58}Ni is not visible at all in the other nucleus. A resonance at 13 MeV also rises faster than the $E2$ resonance in both nuclei, but appears to be weaker in ^{60}Ni than in ^{58}Ni, similar to the one at 7 MeV. The pointed peak of the main bump at 16 to 18 MeV becomes flatter with rising angle, thus indicating the existence of higher multipolarities. A resonance at 27 MeV rises somewhat, but not dramatically, faster than the resonance at 32 MeV.

In addition, the ^{60}Ni spectra show a resonance at 40 MeV. All lines drawn in Figs. 5 and 6 had to be included in the fit to achieve a reasonable χ^2. Omission of any of them made a consistent fit of all spectra impossible.

B. Distribution of $E1$ strength

We believe our measurement to be the first measurement of the total $E1$ strength between 10 and 30 MeV in ^{58}Ni and ^{60}Ni. In light nuclei up to approximately calcium the total cross sections have been measured directly through real photon absorption,[26] but for heavier nuclei the radiative corrections become very large and introduce a large uncertainty. The total $E1$ cross section for heavy nuclei is given by the neutron production cross section. It is the intermediate region with $40<A<90$ which poses problems. Short of summing up partial cross sections with the inherent difficulty of possible double counting, as e.g., the (γ,pn) cross section in both the (γ,n) and the (γ,p) channels, (e,e') seems to be the best method for measuring directly the total $E1$ cross section. In addition, the (γ,p) measurements do not generally have the accuracy achieved in the (γ,n) work and (e,p) measurements at present can only be evaluated using virtual photon DWBA calculations for point nuclei.[27]

However, there is information on the distribution of dipole strength in the particle channels from (γ,n), (γ,p), and capture reactions. The proton and neutron channels especially have been investigated by numerous experiments. Many of these measurements were initiated by the observation that the neutron production cross section in ^{58}Ni and ^{60}Ni is different by about a factor of 2.[3] In summary, all recent experiments agree insofar as only 30 to 35% of the classical $E1$ sum rule [Thomas-Reiche-Kuhn (TRK)[28]] are found in the (γ,n) cross section between 10 and 30 MeV in ^{58}Ni, but 70% in ^{60}Ni (Refs. 5, 29); the (γ,p) (Ref. 30) and (e,p) (Refs. 31, 32) cross sections have been measured to be such that if added to the (γ,n) value give comparable total cross sections in both nuclei. In Table II we have assembled some results from those experiments which investigated both nuclei. All sum rule percentages correspond to integration from 10 to 30 MeV, with the exception of the (e,p) measurement of Ref. 32 which extends to only 26 MeV, and which, therefore, should have the smallest integrated cross section. More information concerning previous experiments and numerous graphical presentations of experiments and theory can be found in Ref. 5.

The cross section at 45° from the present experiment is shown in Fig. 7. The amount of $E2$ strength is indicated. Other multipolarities are negligible. In the bottom part of Fig. 7 the relative distribution of the $E1$ strength—the $E2$ was found to be practically identical in both nuclei—is compared. Since in (e,e') the cross sections are only indirectly representative of the absolute strength, the ^{60}Ni cross section has been renormalized so that the peak cross sections are equal. It is evident that the strength in the peak area is shifted downwards by going from the $T=1$ to the $T=2$ nucleus. Integrated sum rule percentages

TABLE II. Some results from different reactions for ^{58}Ni and ^{60}Ni selected from experiments which investigated both isotopes. They clearly show the tendency described in the text: (γ,p) and (γ,n) values add up to about 90 to 100% EWSR in both isotopes. In addition to the experiments quoted, there is another one which investigated both nuclei—inelastic scattering of 200 MeV electrons by Gulkarov[38] which, however, has been evaluated in plane-wave Born approximation (PWBA) and not DWBA and might, therefore, be misleading. The agreement between the resonance parameters, but not strength, extracted by a line shape fit from the ^{60}Ni (γ,n) data of Ref. 5 and ours should be noted because it indicates that ~20% of the ^{60}Ni cross section could be in the (γ,pn) channel. The errors quoted for this work are those from statistical uncertainty only. Since the full error matrix was evaluated in the χ^2 fit, this includes contributions from the error of the background parameters. In particular, no uncertainty from model dependency was taken into account.

			^{58}Ni			^{60}Ni		
Method	E^{max}(MeV)	Ref.	E_x(MeV) [a]	Γ (MeV)	R (%) [b]	E_x(MeV) [a]	Γ (MeV)	R (%) [b]
(γ,n)	30	29	21.9 ± 0.3 [c]		36 ± 4 [d]	20.7 [c]		69 ± 6 [d]
(γ,n)	33.5	5	17.3		29 [e]	16.3	2.44	11 [e]
						18.51	6.37	62 [e]
(γ,p)	30	30	21.4 ± 0.3 [c]	10	66 ± 7 [d]			36 [d]
(e,p)	26	26	20.6		55 ± 12 [d]	21.1 [c]		23 ± 9 [d]
(e,p)	50	32	19.2 ± 0.5	6.5 ± 1.3	83 ± 5 [e]	18.5 ± 0.5	9.2 ± 1.8	33 ± 2 [e]
(e,e')		Present work	17.5 [f]		95 ± 10 [e]	16.2 [f]		89 ± 10 [e]

[a] Fitted resonance energy if not indicated otherwise.
[b] $R = E_x B(E1)/[(9\hbar^2/8\pi M)\cdot(NZ/A)]$ (Thomas–Reiche–Kuhn sum rule), M = proton mass.
[c] Energy defined by $E = \int_0^{E^{max}} E\gamma\sigma dE\gamma / \int_0^{E^{max}} \sigma dE\gamma$.
[d] Integrated from lowest to highest measured point.
[e] Integrated from 10 to 30 MeV.
[f] E_x of peak.

and the detailed parameters for the four resonances needed to describe the overall shape of the cross section are given in Table III. The summed strength is compared to the DWBA calculations in Fig. 9. The curves for various models have been normalized to the 45° (0.37 fm^{-1}) data. The MS model describes the data best, but there is a small systematic raise at higher momentum transfer, which may be due to higher multipoles not separated by the line shape fit. For ease of comparison the strength corresponding to integration from 10 to 30 MeV is given in Table III together with the value from integration to infinity.

Table IV shows the sum of proton and neutron cross sections and compares it with the total (e,e') cross section of Table III. For σ_n the average of Refs. 5 and 29, 33% and 71% EWSR, was used. The sum of $\sigma_n + \sigma_p$ should be equal to or larger than the total cross section as measured with (e,e'), because the (γ,pn) cross section would be counted in both channels. The three sets of data in Table II are consistent with this condition

TABLE III. Strength of $E1$ components in the present work. The resonance parameters shown were used to approximate the $E1$ strength distribution for the χ^2 fit. As evident from Fig. 8, where mainly $E1$ contributes, the $E1$ strength function is reasonably well described. The $E1$ strength extracted from the resonances, corresponding to integration to infinity, adds up to approximately 110% of the classical $E1$ sum rule. For ease of comparison, we also give the sum rule strength found by integration from 10 to 30 MeV, 94 ± 10 and 87 ± 10% for ^{58}Ni and ^{60}Ni, respectively. The table and Fig. 8 also show that the peak strength is shifted to lower excitation energy by going from ^{58}Ni to ^{60}Ni. Although the gross shift is in agreement with the isospin coupling model[1,37] we do not think it is a sufficient basis for a claim of observed isospin splitting. The average excitation energy, weighted with the $E1$ strength function between 10 and 30 MeV, in contrast, remains virtually unchanged.

		^{58}Ni					^{60}Ni		
E_x(MeV)	Γ (MeV)	B (fm^2)	$R\gamma$ [a]	R_∞ [b]	E_x(MeV)	Γ (MeV)	B (fm^2)	$R\gamma$ [a]	R_∞ [b]
13.1 ± 0.3	1.4 ± 0.5	0.4	2.3	2.5 ± 1	12.65 ± 0.3	1.5 ± 0.4	0.9	4.5	5 ± 1
16.2 ± 0.3	2.5 ± 0.5	1.5	10.5	11 ± 2	16.6 ± 0.4	2.75 ± 0.5	2.5	16.5	18 ± 4
18.3 ± 0.5	4.5 ± 0.5	7.3	54	62 ± 7	19.5 ± 0.5	6.0 ± 1.0	7.4	51	63 ± 8
22.0 ± 1.0	6.0 ± 1.0	3.3	27	34 ± 8	23.5 ± 1.5	6.0 ± 1.5	1.9	15	19 ± 4
			94	110 ± 11				87	105 ± 10

[a] $\int_{10}^{30} (dB/dE_x)(dE_x/\text{EWSR}\,100)$.
[b] $E_x B(E1)/\text{EWSR}\,100$.

TABLE IV. Total $E1$ cross sections in ^{58}Ni and ^{60}Ni. For the neutron and proton cross section measurements the total cross section has been defined as $\sigma_n + \sigma_p$, thus neglecting complications (double counting of σ_{np}). The average value from Refs. 5 and 29, 33% and 71% of the $E1$ EWSR, was used for σ_n in ^{58}Ni and ^{60}Ni, respectively.

Reference used for ($\gamma_1 p$) cross section	S for ^{58}Ni	S for ^{60}Ni
30	99	107
31	97[b]	103[b]
32	116	104
Present work	94	87

[a] $S = (\sigma_n + \sigma_p)/\sigma_{TRK}$ for photons; $S = \int_0^{30} dE_x dB/dE_x/\text{EWSR}$ 100 for (e, e').

[b] Estimated corrected value for integration to 30 MeV.

and with each other with the possible exception of the (e,p) result from Ref. 32 for ^{58}Ni. If we interpret the difference between the cross section in the partial channels (average of the three measurements of Table III) and the total cross section as indicative for $\sigma(\gamma,pn)$, up to approximately 10% and 20% of the sum rule are possible in this channel in ^{58}Ni and ^{60}Ni, respectively, between 10 and 30 MeV.

Before we try to interpret the distribution of total $E1$ strength we want to review the main features of the isospin coupling model mentioned above. This model, developed by Goulard and Fallieros,[1] predicts that in nuclei with ground state isospin $T_0 = 0$ and $T_3 = T_0$, isovector ($\Delta T = 1$) excitations with $\Delta T_3 = 0$ can lead to states with isospin T_0 and $T_0 + 1$, named $T_<$ and $T_>$, respectively. The neutron decay of the $T_>$ states to low-lying levels in the daughter nucleus is forbidden because the neutron would have to carry away $\Delta T = \frac{3}{2}$. The proton decay of the $T_<$ states is claimed to be inhibited by the Coulomb barrier. Based on these considerations, the $T_>$ states have generally been identified with the (γ,p) process and vice versa; the $T_<$ states and the (γ,n) cross section were connected similarly.[33-36]

For the isotope pair ^{58}Ni ($T_0 = 1$) and ^{60}Ni ($T_0 = 2$) differences between the strengths of $T_>$ and $T_<$ states should be maximal, making it a very suitable choice for the observation of isospin effects. The $T_>$ states are predicted to be higher in energy than $T_<$ by an amount $\Delta E = V(T_0 + 1)/A$ (Ref. 37), with $V = (58 \pm 5)$ MeV determined experimentally in the nickel region,[2] corresponding to $\Delta E(^{58}\text{Ni}) = 2.0$ MeV and $\Delta E(^{60}\text{Ni}) = 3.1$ MeV. Shell model calculations for nickel show the (γ,n) and (γ,p) states to be not clearly separated although the average excitation energy of the (γ,p) states is approximately 2 MeV higher than the (γ,p) states, thus agreeing with the isospin coupling model.[33,34]

The ratio of transition strengths $I_>/I_<$ is predicted by the isospin coupling model[6] to be 0.80 for ^{58}Ni and 0.36 for ^{60}Ni. Clearly the ratio of the (γ,p) to (γ,n) cross section for ^{58}Ni and ^{60}Ni, 2 and 0.5, respectively (Table I) is not in quantitative agreement with this prediction for ^{58}Ni. One explanation is the possibility of intermediate neutron decay of the $T_>$ states in ^{58}Ni and ^{60}Ni through high-lying $T = \frac{3}{2}$ and $T = \frac{5}{2}$ states, respectively, in the daughter nuclei.[5] In summary then, one might conclude that the magnitude of photonuclear cross sections in ^{58}Ni and ^{60}Ni, though strikingly different in different channels, can be explained qualitatively by the schematic macroscopic isospin coupling model.

A closer look at the microscopic calculations[33-36] shows that the picture is more complicated. The calculations by Ishkanov *et al.*[36] and Tanaka,[33] which investigate the branching ratios as well as the position and strength of T_0 and $T_0 + 1$ states, show that the proton and neutron emission compete with each other for both $T_<$ and $T_>$ states and depend sensitively on the amount of 2 or 4 particle components. Tanaka not only calculates $T_<$ and $T_>$ states, but also the cross sections for ^{58}Ni (γ,n) ^{57}Ni, ^{58}Ni (γ,p) ^{57}Co, ^{60}Ni (γ,n) ^{59}Ni, and ^{60}Ni (γ,n) ^{59}Co.

There is no one to one correspondence between $T_<$ and (γ,n), and $T_>$ and (γ,p). The calculations show large deviations for ^{58}Ni from the rule that $T_<$ states decay by neutron emission and $T_<$ by proton emission. While the first deviation may not be too surprising because the $T_<$ at 17 MeV is 7 MeV above the proton Coulomb threshold, the neutron decay of $T_>$ is surprising, but may be explained as proceeding through high-lying analog states in the daughter nuclei. In ^{58}Ni proton emission is dominant from the $T_<$ state around 17 MeV, but neutron emission is dominant in the case of ^{60}Ni. Neutron and proton decay compete with each other from the $T_>$ states in both nuclei. Consequently shapes and strength of the photoparticle cross sections are different. In ^{58}Ni the photoneutron component from the $T_<$ is suppressed, but is relatively large from the $T_>$ (where it should be forbidden by the isospin coupling model); this makes the photoneutron cross section spread out very much.

The calculations by Ngo-Trong and Rowe[34] agree roughly with those of Tanaka[33] in strength and position of $T_<$ and $T_>$ states, but have not been extended to include branching ratios. However, the positions of the various parts of the dipole strength agree quite well with the ex-

TABLE V. $E2$ strength at 16 MeV in ^{58}Ni.

E_x	Γ	R [a]	Reaction	Ref.
16.3	≈4.5	57 ± 6	(e,e')	53
16.5	4.2 ± 0.5	50 ± 10	$(\vec{p},p')$	54
16.0 ± 0.5	4.5 ± 0.3	50 ± 10	(d,d')	59
16.4 ± 0.3	4.9 ± 0.2	55 ± 15	(α,α')	17
16.5		≈50	$(\vec{p},p')$	55
~16	~3	4.3	^{54}Fe$(\alpha,\gamma)^{58}$Ni	43
16.5 ± 0.5	4.2 ± 1.0	56 ± 4	(e,α)	32
16	3.2	40 ± 15	$(^{16}O,^{16}O)$	67
16.2 ± 0.3	4.5 ± 0.4	65 ± 10	(e,e')	Present work

[a] $R = E_x B(E2)/\mathrm{EWSR}(E2,\ \Delta T = 0)\ 100$.

perimental data from this experiment (Table III).

Isospin effects have also been investigated through a reanalysis[35] of the 200 MeV (e,e') data of Gulkarov *et al.*[38] Originally these data, which show distinct structure at 13, 16, and 28 MeV, have been analyzed in the framework of the dynamic collective model (DCM), which couples the dipole oscillation to low energy quadrupole oscillation,[39] and were found to verify the predictions of the DCM. No experimental evidence has been upheld for the DCM until now (see, e.g., Ref. 40). Similarly, revisions of the (e,e') evaluation by Gulkarov[41] later interpreted the resonance at 13 MeV as *the* giant quadrupole state and the bulk strength at 16 MeV as *the* giant dipole resonance. On this basis the data above 14 to 15 MeV, believed to contain only $E1$ strength, were recently[35] interpreted as evidence for isospin splitting, despite the rather large momentum transfer of the data used ($q \gtrsim 0.7$ fm^{-1}). At this momentum transfer $E2$ strength dominates the 16 MeV region.

From our data the following conclusions may be drawn: (1) The isospin splitting model agrees with the data in both nuclei only insofar as the total strength is shifted downwards. Identification of $T_<$ with (γ,n) and $T_>$ with the (γ,p) cross section is not corroborated. (2) The distribution of $E1$ strength is rather accurately described by shell model calculations, which also account quantitatively for the photoproton and photoneutron cross sections measured. (3) The total $E1$ strength in both Ni isotopes investigated is equal within errors.

C. Isoscalar $E2$ strength at 16.5 MeV

There have been a large number of experiments investigating the 16 MeV region of ^{58}Ni; a few have also investigated ^{60}Ni. For convenience of comparison, those ^{58}Ni measurements which give a quantitative result for the $E2$ strength are shown in Table V; measurements in both nuclei are compared in Table VI. Most of the results agree insofar as 50 to 65% of the EWSR ($\Delta T = 0$) are found in both nuclei. Our data, shown in Fig. 10, are consistent with these numbers.

Similar to the $E1$ resonance, there is a question of how this strength is distributed into particle channels. The conclusion from (e,α) measurements[32] that all, or nearly all, of the resonant $E2$ strength is in the α channel has been doubted on the basis of $(\alpha,\alpha'n)$, $(\alpha,\alpha'p)$, and $(\alpha,\alpha'\alpha)$ experiments[42] together with the ^{54}Fe (α,γ) ^{58}Ni results (Ref. 43). The isoscalar strength in the p

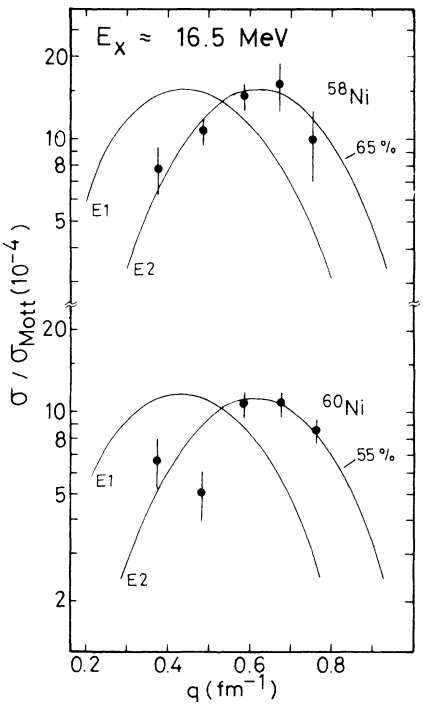

FIG. 10. Comparison of the experimental cross section with DWBA calculations for the resonance at 16.2 MeV. The $E2$ curve, calculated with the Goldhaber-Teller model, fits best.

TABLE VI. Comparative measurements of ^{58}Ni and ^{60}Ni for the $E2$ resonance.

^{58}Ni			^{60}Ni				
E_x(MeV)	Γ (MeV)	R [a]	E_x(MeV)	Γ (MeV)	R [a]	Ref.	Method
16.4 ± 0.3	4.9 ± 0.2	55 ± 15	16.6 ± 0.3	5.0 ± 0.4	63 ± 15	17	(α,α')
16.5 ± 0.5	4.2 ± 1.0	56 ± 4	16.0 ± 0.5	3.7 ± 0.8	52 ± 3	32	(e,α)
16.2 ± 0.3	4.5 ± 0.4	65 ± 10	16.3 ± 0.3	4.5 ± 0.4	55 ± 10	Present work	(e,e')

[a] $R = E_x B(E2)/\mathrm{EWSR}(E2, \Delta T = 0)$.

channel was found to be about five times the strength in the α channel. In addition, a sizable neutron decay branch was found. As mentioned in connection with the measurement of the GDR, electroexcitation suffers from the limitation to point nuclei in the DWBA formalism. In the case of the $E2$ absorption the neglect of $E3$ (and higher) multipoles could also seriously effect the results.

While the partial $E2$ cross sections still have to be established, the total $E2$ cross sections seem to be inproblematic. Not only do different methods agree, the excitation energy conforms to the rule established from measurements in other nuclei, $63\,A^{-1/3}$ MeV. The strength, though lower than in heavier nuclei, agrees with the trend found from measurements over a wide range of nuclei, namely, an apparent reduction in strength as measured in percentages of the isoscalar $E2$ sum with A.[15]

While the reduction in strength has not been predicted by calculations, the excitation energy has been predicted to $\approx 60\,A^{-1/3}$ MeV by the Bohr-Mottelson self-consistent shell model.[24,25,44]

D. High energy bound octupole states (HEBOS)

In the general framework described in Sec. IV A and quantified on the basis of the calculations of Ref. 25 in Table I, isoscalar octupole strength is expected at $25\,A^{-1/3}$ MeV. It has been known for a long time that there are strong octupole states at much lower energy levels, in fact, in double magic nuclei they are the lowest levels. Although higher-lying $E3$ states are known from (e, e') (see, e.g., Table 27 in Ref. 45), only recently have they been investigated in a systematic manner.[9,15] The inelastic α scattering experiments,[9] especially, covered many nuclei ranging from ^{40}Ca to ^{208}Pb. To summarize, $E3$ strength was found to cluster around $30\,A^{-1/3}$ MeV, but to be distributed quite differently in spherical and deformed nuclei. But this $E3$ strength is not concentrated in a form which looks like a resonant excitation. It has been shown[10] in (e, e') for ^{89}Y that the strength weighted excitation energy of all low-lying octupole states is close to the value predicted.[25] In spherical nuclei the response function is well described[9] by more sophisticated RPA calculations.[46-48] There are important discrepancies between (α, α') and (e, e') (Ref. 49) for ^{208}Pb; these have been described recently.[7] Only better (e, e') experiments will be able to solve this problem.

Concerning the present paper, the lowest particle thresholds for proton decay are $E_x = 8.2$ and 9.5 for ^{58}Ni and ^{60}Ni, respectively. The concentration of $E3$ strength found in our measurement is clearly below these thresholds and these states are bound states. Not surprisingly, the distribution of strength is quite different in the two nuclei (Figs. 5 and 6). Owing to the limited resolution of this experiment, more $E3$ strength may be hidden under the peaks at 6 MeV in both nuclei. While the HEBOS strength in ^{58}Ni is concentrated

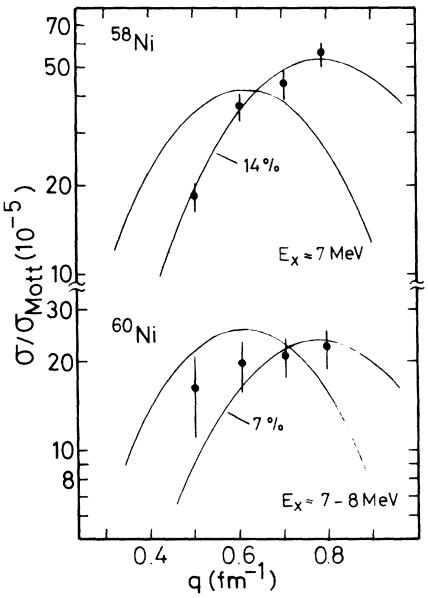

FIG. 11. Comparison of experimental cross sections for a state (group of states?) at 7 MeV in ^{58}Ni and a broup of states between 7 and 8 MeV in ^{60}Ni with DWBA calculations. The ^{58}Ni data follow an $E3$ form factor quite well, but the ^{60}Ni data, which carry only half of the ^{58}Ni strength, may include an $E2$ or $E1$ contribution.

into states within 1 MeV (width of the enveloping curve) of $E_x = 7$ MeV and comprises 14% of the EWSR ($E3$, $\Delta T = 0$), only 6% could be localized in ^{60}Ni (Fig. 11) and even this strength is spread out over a wider range of excitation energy. Since the 6 MeV state(s) is at the end of our spectra and nothing is known about the (clustering) width, we did not try to decompose the peaks which are clearly visible at 6 MeV in Figs. 5 and 6. An additional 8.5% of the EWSR is carried in ^{58}Ni by the lowest $E3$ state at 4.5 MeV,[50,51] and in ^{60}Ni by two states at 4 MeV (Refs. 51, 52) and 6.2 MeV.[52]

E. Resonant cross section around 13 MeV

Distinct resonant excitations of the nuclear continuum at 13 ($51\,A^{-1/3}$) MeV in ^{58}Ni, ^{60}Ni, and ^{64}Ni were first reported in the inelastic scattering of 200 MeV electrons from the Karkov accelerator by Gulkarov *et al.*[38] The experiments were part of an effort to find the surface quadrupole excitations coupled to the giant dipole resonance, as predicted by the collective dynamic model.[39] After the discovery that a giant quadrupole resonance existed as a genuine property of the nuclear continuum, a re-evaluation of the data in Born approximation identified the 13 MeV resonance in all three isotopes as $E2$ (Ref. 41) (in fact, it was believed to be *the* main quadrupole GR). Other experiments which find structure at this energy [$\sim(50-53)\,A^{-1/3}$ MeV] in nuclei with $56 \lesssim A \lesssim 60$ partly support and partly contradict an $E2$ assignment.

Torizuka *et al.*[53] found two $E2$ (or $E0$) states with a width smaller than 0.6 MeV at 13.2 MeV and 14.0 MeV in ^{58}Ni, which exhaust 7.4 ± 0.7 and 4.8 ± 0.7% of the isoscalar energy weighted quadrupole sum rule [($E2$, $\Delta T = 0$) EWSR]. Similarly, polarized proton measurements favor $E2$ (or $E0$), while ruling out $E3$.[54,55] Inelastic ^{3}He scattering on ^{48}Ti, ^{56}Fe, ^{59}Co, and ^{60}Ni by Arvieux *et al.*[56] consistently found a peak with width $\Gamma \approx 1.2$ MeV at $51\,A^{-1/3}$ MeV (13 MeV in ^{60}Ni) for which an $E2$ assignment was the most probable, but an $E4$ could not be ruled out. However, in 155 MeV proton scattering[57] and 250 MeV electron scattering[58] on ^{56}Fe a peak around 13.5 MeV has (tentatively) been assigned $E3$. The report on inelastic scattering of deuterons,[59] while not giving an assignment, shows in the spectra that the angular behavior of the cross section of a state at 13 MeV is different from the $E2$ ($\Delta T = 0$) giant resonance at 16 MeV. Inelastic α scattering finds several multipolarities present,[17] but not $E2$ (Ref. 43).

The existence of a resonance 13 MeV up in the continuum with a width of only (1–2) MeV is exciting enough. Even more importance comes to this state at $51\,A^{-1/3}$ from the observation in (e, e'), and only in (e, e'), of a state at approximately the same energy (in $A^{-1/3}$ MeV) in many nuclei between $139 < A < 208$, which, consistent in all experiments, has been assigned either $E2$ or $E0$ (Refs. 7, 15) multipolarity. [See, e.g., Ref. 60 for the well-known difficulties in discriminating $E2$ and $E0$ in (e, e').] Since the existence of a second giant quadrupole resonance in the continuum below the $63\,A^{-1/3}$ MeV mode seems unlikely (but not impossible), the $53\,A^{-1/3}$ MeV state has been regarded as a serious candidate for the giant monopole (breathing mode) resonance.[61] On the other hand, $52\,A^{-1/3}$ MeV is the energy predicted by Hamamoto[25] for the isovector $E3$ ($1\hbar\omega_0$) state, based on the Bohr-Mottelson self-consistent shell model and the strength found in ^{89}Y fits the predicted characteristics.[10] Recently, this state has been proposed to be an isovector quadrupole oscillation of the excess neutrons in nuclei with $A > 90$ (Refs. 7, 15).

The situation seems to be difficult to understand because in general the various continuum modes discovered since 1971 have exhibited a very smooth dependence on the nuclear mass A, and resonances at the same energy (again in $A^{-1/3}$ MeV) in different nuclei have been found to be of the same multipolarity. Therefore, we thought it of the utmost importance to investigate the $53\,A^{-1/3}$ MeV mode in nuclei with $A < 139$. However, a first experiment on ^{89}Y, surprisingly,[10] did not show any resonant $E2$ cross section around $53\,A^{-1/3}$ MeV which would be compatible with the strength found in heavy nuclei.[7,15]

The momentum transfer dependence for resonances at this energy in both isotopes is shown in Fig. 12, which compares the experimental values to DWBA calculations on the basis of the hydrodynamical model. It has already been mentioned that the 13 MeV complex in Fig. 5 (^{58}Ni) seems to rise faster and higher as compared to Fig. 6 (^{60}Ni). This is borne out by Fig. 12. It is clear that the disentangling into multipolarities is somewhat ambiguous. However, Fig. 12 rules out any sizable $E4$ contribution, while $E2$ was not considered, based on Refs. 17 and 43, for the results presented. Even if $E2$ is considered its contributions are less than 4% EWSR for ^{58}Ni and 3% for ^{60}Ni. The $E3$ strength inferred from Fig. 12 is much larger than the 2% predicted for isovector $1\hbar\omega_0$ $E3$ strength from Table I.

But the large difference between the two nuclei already indicates a great sensitivity to the nucleon configurations present and less sensitivity to the macroscopic properties mainly proportional to A. The $E1$ strength found compares quantita-

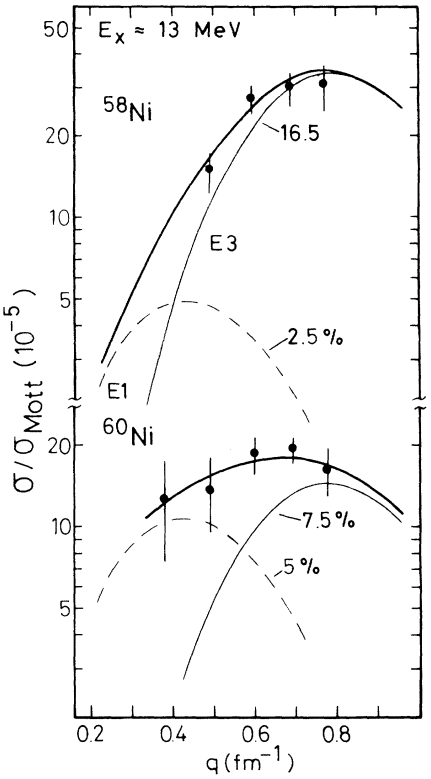

FIG. 12. Comparison of experimental to DWBA cross sections for states (group of states?) at around 13 MeV. The cross section in ^{58}Ni is clearly of pronounced resonant structure (see Fig. 5). While there is cross section visible in ^{60}Ni, it is not as strong as in ^{58}Ni (see Fig. 6). Following Ref. 43 we have not included the $E2$ cross section in the disentangling of the form factor (see text for more details).

tively favorably to the shoulder found in photon work at 13 MeV (compare, e.g., Fig. 7 with the composite figures of Ref. 5).

The $E3$ assignment for the predominant mode of excitation at 13 MeV creates a problem because of the contradicting assignments quoted above. However, critical analysis of the data shows that the statistical uncertainties are quite large,[56,57] that the assignment rests mainly on two low points in the spectrum at the highest momentum transfer,[53] or that other problems have been encountered (see, e.g., remark in Ref. 4 of Ref. 59). In addition, nearly all papers call their assignment tentative or do not quote any strength. Although the excitation energy agrees closely with the 52 $A^{-1/3}$ MeV predicted,[25] this state cannot be isovector owing to its strong appearance in (d,d') spectra[59] and its strength being a factor of 5 too large when compared to Hamamoto's results.

On the other hand, the argument that isoscalar D and α scattering does not excite isovector states has been doubted recently.[7,32] Probably coincidence measurements would be the best way to decide which multipolarities, and how much strength for each, are hidden in this complex. In any case, one may conclude that in medium-heavy nuclei the $E3$ strength is more fragmented than in heavy nuclei, which may enable one to learn more about the octupole-octupole interaction in nuclei from giant resonances than has to date been possible from the very regular appearance of the quadrupole states for the quadrupole-quadrupole interaction.

F. $3\hbar\omega_0$ isoscalar octupole strength

From the schematic model (Table I) and the systematics of heavier nuclei (Figs. 13, 21, and 22 in Ref. 7) one would expect octupole strength at 28 MeV with a width of 8 MeV and a strength of 20 to 30% of the EWSR ($E3$, $\Delta T = 0$). (The strength given for nickel in Fig. 21 of Ref. 7 is from a preliminary analysis and somewhat lower than the value given here.)

In the Ni isotopes investigated we find a resonance at 27 ± 1 MeV with a width of 7 ± 1.5 MeV. In Fig. 13 the cross sections of this resonance are compared to $E2$ and $E3$ DWBA calculations. An $E3$ assignment is favored and leads to 52 ± 15

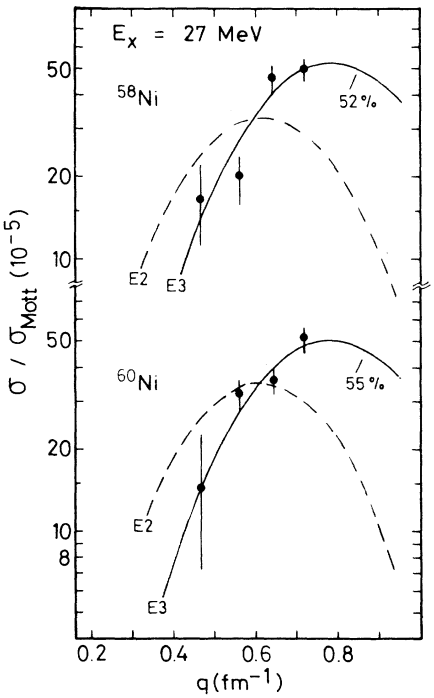

FIG. 13. Comparison of experimental and DWBA cross sections for resonance at 27 MeV. An $E3$ assignment is preferred and leads to about equal strength in both nuclei.

and 55 ± 15% EWSR ($E3$, $\Delta T = 0$) for ^{58}Ni and ^{60}Ni, respectively.

The strength extracted is higher than in other heavier nuclei.[7,10] This does not necessarily mean that there is less $E3$ strength around 110 $A^{-1/3}$ MeV in the other nuclei. One reason might be that the $E3$ strength is more concentrated in the Ni isotopes. Another contributing factor may rest with the background form chosen. Due to the improvement in radiation tail calculations we were able to drop the scaling parameter for the radiation tail (term P_3 in the equation for BGR in Sec. III A of Ref. 10). Although the scaling always was small, that is, P_3 close to one, we noted a systematic tendency to lower values at backward angles. This leads to a flatter background. Applying the background without scaling to the ^{89}Y data[10] we found in a reanalysis 40% of the EWSR ($E3$, $\Delta T = 0$) instead of the 20% estimated[10] for the region between 22 and 26 MeV in ^{89}Y. The values of the other resonances, which show up in resonant form, were essentially unchanged with the exception of the GDR at the higher angles. However, a change in strength for the GDR would be approximately compensated by using the Myers-Swiatecki instead of the Goldhaber-Teller model.[7]

In summary, we found approximately 55% of the isoscalar $E3$ strength concentrated in the main $3\hbar\omega_0$ mode at 27 MeV. Together with low-lying $E3$ states (24 and 16% for ^{58}Ni and ^{60}Ni) and some possible strength higher up (see below), a large part of the $E3$ strength expected from the sum rule has been found to be localized; the remainder is probably spread out over a wider range of excitation energy.

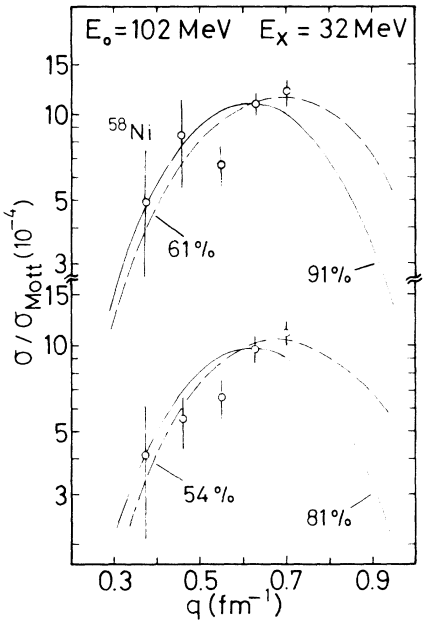

FIG. 14. Comparison between experimental and DWBA cross sections for resonance at 32 MeV. An $E2$ assignment is preferred, but other multipolarities (not taken into account) could contribute. The Goldhaber-Teller model leads to the higher strength; this strength might be regarded as an upper limit. The Myers-Swiatecki model (broken line) assumed $\alpha = 1$ (see text for definition). Extension of the Myers-Swiatecki model by Kodama to higher multipolarities gives values for α ranging from 0.12 to 0.44. Thus the sum rule values given in the figure for the MS model should be regarded as lower limits. The dependence of the experimental points on the momentum transfer suggest the possibility of more than one multipolarity contributing. This possibility was not investigated due to the accuracy limitations at this high excitation energy.

G. Isovector $E2$ strength at 32 MeV

The isovector part of the $E2$ strength at ~130 $A^{-1/3}$ MeV, discovered together with the isoscalar resonance,[62] is much less well investigated than the 63 $A^{-1/3}$ MeV resonance. This is due to two causes: First, this resonance is further up in the continuum and has, therefore, not only a larger total width, which reduces its peak cross section, but furthermore, the sum rule limit is exhausted by smaller reduced transition probabilities. Second, as an isovector state it is not as strongly excited by hadron scattering as the isoscalar $E2$ GR. Consequently, it has only been investigated in some detail by capture reactions and electron scattering.

Similar to the isoscalar strength, as A becomes smaller a smaller fraction of the sum rule is concentrated in a resonance. While for light nuclei at least some resonancelike concentration for the isoscalar state has been found for ^{28}Si, the isovector part seems to be spread out more or less from 23 to 42 MeV.[63]

The isovector resonance in ^{58}Ni and ^{60}Ni is clearly visible in Figs. 5 and 6 at 32 ± 1 MeV. A width of 10 ± 1.5 and 9 ± 1.5 MeV for ^{58}Ni and ^{60}Ni, respectively, is deduced from the line shape fits. The experimental cross sections are compared in Fig. 14 with DWBA calculations. Two models have been used. The Goldhaber-Teller model leads to a strength of 91 ± 18 and 81 ± 16% of the EWSR ($E2$, $\Delta T = 1$) (solid line), the Myers-Swiatecki model to 61 ± 12 and 54 ± 11% (broken line). In the case of the Myers-Swiatecki model, which fits the experimental points better, the ratio α of GT flow to SJ flow (see Sec. IV B) has been assumed to be $\alpha = 1.0$. Quantitative extensions of the Myers-Swiatecki model[23] by Kodama[64] for the case of $E2$ gives $\alpha = 0.29$ for the droplet mode. It is interesting to note that for the $E2$ mode the

contribution of the SJ mode, a volume oscillation, is diminished in comparison to the dipole case. This is exactly what one would naively expect from higher multipoles, which will be more and more pure surface oscillations.

It appears from the strength found here and the strength in ^{89}Y that possibly the isovector strength is more concentrated in one resonance than the isoscalar state. For the dipole mode it was found a long time ago that within the schematic model the strength is pushed into the highest available levels.[65] The schematic model of Hamamoto predicts the same for $E3$ and $E4$ isovector strength and the more elaborate RPA calculations give the same picture.[46-48] The systematic fitting errors, discussed in Sec. III, are rather large for the high-lying states and preclude a definite statement. However, it is clear that the strength of the isovector states are of fundamental importance and deserve further consideration.[24]

H. Hexadecupole strength

There have been no clear, if any, assignments of $E4$ multipolarity for continuum transitions, although many calculations predict sizable strength underlying the isoscalar quadrupole resonance.[25,46-48,66] This is understandable. In hadron scattering an $E4$ cross section would have an angular dependence in phase with $E2$. In electron scattering it only will reach a magnitude suited for measurements at higher momentum transfer.

Similar to the $E3$ states, $E4$ transitions into the continuum are fragmented into four groups (isoscalar and isovector, and these into $2\hbar\omega_0$ and $4\hbar\omega_0$ transitions). Since they are higher in excitation energy than the $E3$, they are spread out over a wider range in excitation energy while smaller cross sections will exhaust the sum rule. The predictions of the schematic model were shown in Table I. Other more complicated calculations[46-48,66] agree in the distribution of the main (resonant) strength.

To determine a multipolarity with certainty one should measure the momentum transfer to at least the maximum of the form factor. As Fig. 1 shows, in our experiment this is not the case for $E4$, and it is difficult to ascertain in the examples discussed below as candidates for $E4$ that it is not partly that $E3$ strength, which is missing in the $E3$ resonances, which shows up. However, $E5$ and higher multipolarities can be ruled out on the basis of strength arguments, since such an assignment would lead to multiple exhaustion of the sum rule. The broken lines in Figs. 5 and 6 represent the resonances proposed to be $E4$. Since the measurement at the two largest angles in ^{58}Ni only went to 41 MeV, a resonance at 40 MeV was assumed to have the same parameters as in ^{60}Ni. This assumption was found to be compatible with the data.

Figures 5 and 6 show the difficulties in extracting $E4$ strength from broad overlapping resonances in (e, e'). Figure 5 shows all the resonances (or concentrations of strength which lent themselves to interpretation and a χ^2 fit with the resonances), the $E1$ having been left out for clarity in Figure 6. It is visible from the ^{58}Ni data in Fig. 5 that even at the highest momentum transfer $E1$ and $E2$ contributions are not small compared to $E4$. Figure 6, where the $E1$ has been left out and the two $E4$ resonances around 17 MeV have been added, shows another peculiarity, namely a dip in the $E4$ cross section at approximately the maximum of the $E2$ resonance. If we would artificially keep the $E2$ cross section at the value corresponding to the lower end of the error interval the dip would nearly disappear. Thus it is

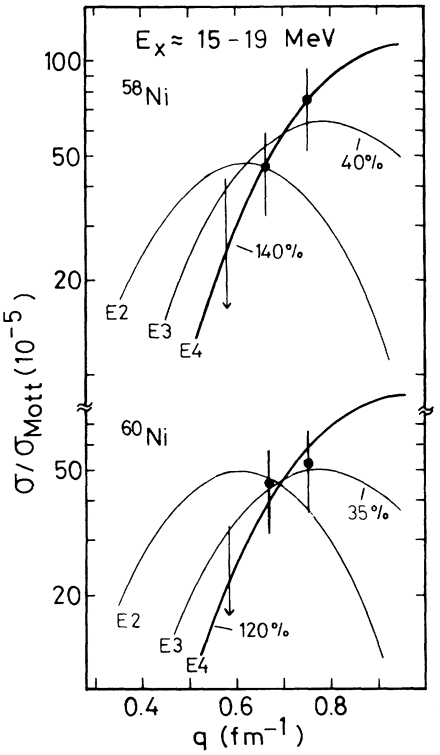

FIG. 15. Comparison of experimental and DWBA cross section in the 13 to 19 MeV region. The experimental values are due to a line shape fit. Figures 5 and 6 show that the bump around 16.5 MeV gets broader going from 75° to 105°. This broadening has to be due to higher multipolarities. Since the assumption of $E4$ alone overexhausts the sum rule by far, other multipolarities have to contribute and the only one possible from the momentum transfer is $E3$ (for more details see text).

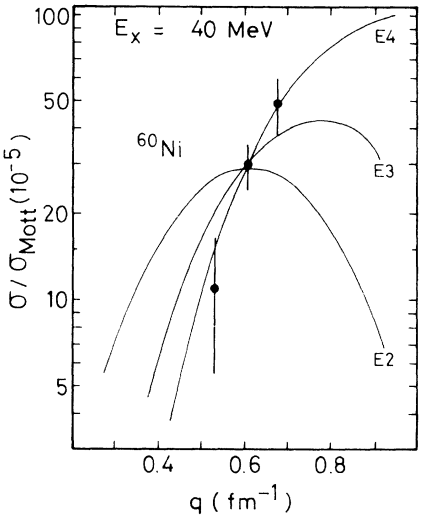

FIG. 16. Comparison of cross section at 40 MeV with DWBA calculations. The experimental points follow an $E4$ curve. These are two problems connected with this resonance. First, it may be doubted that it is real, that is, it may be produced by our special choice of background, because if we add one more parameter to the background function it virtually disappears. Second, it exhausts a rather large fraction of the $4\hbar\omega$ isoscalar strength, namely (150 ± 75)%, compared to the 50% predicted (Ref. 25, Table I).

doubtful that the cross section found in excess of the $E1$ and $E2$ cross section is really that clearly split into two resonances. Figure 15, in addition, shows that an $E4$ assignment, more than exhausting the $E4$ isoscalar sum rule, agrees just as well with the data as an $E3$ assignment. In fact, as mentioned earlier, both might be present. There is also the possibility that transverse $M1$ or $M2$ excitations (magnetic or spin-flip electric) are present in this region. Their angular dependence might mimic the momentum transfer dependence of the higher electric multipole. From Figure 15 one can estimate that the assumption of 15 to 20% of the isoscalar $E3$ strength, present in the region from 15 to 19 MeV, would lead to 50 to 70% of the $E4$ sum rule contributing to the total cross section. The total estimated error in the assignment of the area under the curve we have called $E4$ is 50%.

Figure 16 shows the data points for the 40 MeV structure in ^{60}Ni. It agrees rather well with an $E4$ assignment, although a sizable $E3$ admixture cannot be ruled out. If taken as purely $E4$ it would exhaust 150± 75% of the EWSR ($E4$, $\Delta T = 0$).

There are two more states which have a momentum transfer dependence compatible with $E4$. The rather small peaked structure at 9.6 MeV in ^{58}Ni follows an $E4$ form factor with 5% of the sum rule, but it might as well be $M1$. The form factor of the latter assignment would be on the rising part of its second maximum, thus reproducing the steep rise of $E4$. The same is true for the shoulder at 11.5 MeV in ^{60}Ni (Fig. 6), leading to 3% of the sum rule.

We have recently compared our results for ^{140}Ce with a preliminary analysis of the nickel data (Table IX, Ref. 7). While we have found in our final analysis that the $E4$ strength in Ni at 15 MeV extends higher up and is larger than quoted[7] there still is a certain regularity in terms of $A^{-1/3}$ excitation energy dependence. As in the Ce case, the large uncertainties preclude more definite statements but we hope that our investigation may provoke more work in this area.

V. SUMMARY

The nickel isotopes investigated in this paper have posed unusual difficulties for the interpretation of the nuclear continuum. While the disentangling of the nuclear response function in the giant resonance region is difficult in general, we found it more complicated in ^{58}Ni and ^{60}Ni than in any other nucleus. In light nuclei the higher multipoles are not excited in the range of qR covered by electrons of approximately 100 MeV (Ref. 63). In addition, the strength seems to be widely distributed and disappears in the background. In heavier spherical nuclei, the resonances with lower multipolarity are better separated, but $E4$ resonances have not unambiguously been identified. Since there are many configurations within the shell model available for $E4$, the strength may be very fragmented or it may be hidden under other resonances.[7,66]

To us, the information one can get from the type of experiment described in this paper seems to be limited for the higher (say $\lambda > 3$) multipoles. They are already strongly model dependent on the maximum of the form factor where one has to measure them. In addition, the strength attributed depends on the models used for the underlying lower transitions. Our $E4$ assignments are, therefore, more tentative than is apparent from the use of the preliminary results in Ref. 7.

Since there are also difficulties with $E3$ and isovector $E2$ resonances, we have only tabulated the results for the GDR and the isoscalar $E2$. Conditions and limitations connected with the strength for these states are discussed in the text.

The only way out to achieve greater accuracy in electron scattering may be, but only may be, coincidence experiments together with the simultaneous measurement of the total cross section. Measurements of the type $(e, e'x)$, however, will

be very time consuming due to the relative weakness of the electromagnetic interaction. This will be true even with high current accelerators because of limitations in target thickness and the many in-plane and out-of-plane angular combinations necessary to unambiguously determine the components of the total strength function. It appears that this problem does not exist for light ion inelastic scattering, where angular momentum matching conditions are very selective.[67]

ACKNOWLEDGMENT

This research was supported in part by the National Science Foundation and the Naval Postgraduate School Research Foundation.

---

*Present address: 13C Escondido, Stanford, California 94305.

†Now at Varian Associates, Palo Alto, California 94303.

[1]S. Fallieros, B. Goulard, and R. H. Venter, Phys. Lett. 19, 398 (1965); B. Goulard and S. Fallieros, Can. J. Phys. 45, 3221 (1967); B. Goulard, T. A. Hughes, and S. Fallieros, Phys. Rev. 176, 1345 (1968).

[2]P. Paul, J. F. Amann, and K. Snover, Phys. Rev. Lett. 27, 1013 (1971).

[3]K. Min and T. A. White, Phys. Rev. Lett. 21, 1200 (1968).

[4]E. M. Diener, J. F. Amann, P. Paul, and S. L. Blatt, Phys. Rev. C 3, 2303 (1971).

[5]S. C. Fultz, R. A. Alvarez, B. L. Berman, and P. Meyer, Phys. Rev. C 10, 608 (1974).

[6]S. Fallieros and B. Goulard, Nucl. Phys. A147, 593 (1970).

[7]R. Pitthan, H. Hass, D. H. Meyer, F. R. Buskirk, and J. N. Dyer, Phys. Rev. C 19, 1251 (1979).

[8]B. L. Berman and S. C. Fultz, Rev. Mod. Phys. 47, 713 (1975).

[9]J. M. Moss, D. R. Brown, D. H. Youngblood, C. M. Rosza, and J. D. Bronson, Phys. Rev. C 18, 741 (1978).

[10]R. Pitthan, F. R. Buskirk, E. B. Dally, J. O. Shannon, and W.H. Smith, Phys. Rev. C 16, 970 (1977).

[11]C. R. Fischer and G. H. Rawitscher, Phys. Rev. 135, B377 (1964).

[12]E. S. Ginsberg and R. H. Pratt, Phys. Rev. 134, B773 (1964).

[13]A. Schwierczinski, Ph. D. thesis, Darmstadt Institute of Technology, 1976 (unpublished).

[14]M. Sasao and Y. Torizuka, Phys. Rev. C 15, 217 (1977).

[15]R. Pitthan, Nukleonika (to be published).

[16]E. F. Gordon and R. Pitthan, Nucl. Instrum. Methods 145, 569 (1977).

[17]D. H. Youngblood, J. M. Moss, C. M. Rozsa, J. D. Bronson, A. D. Bacher, and D. R. Brown, Phys. Rev. C 13, 994 (1976).

[18]A. Migdal, J. Phys. USSR 8, 331 (1944).

[19]M. Goldhaber and E. Teller, Phys. Rev. 74, 1046 (1948).

[20]H. Steinwedel and H. Jensen, Z. Naturforsch. 5a, 413 (1950).

[21]L. J. Tassie, Austr. J. Phys. 9, 407 (1956).

[22]W. D. Myers and W. J. Swiatecki, Ann. Phys. (N.Y.) 55, 395 (1969).

[23]W. D. Myers, W. J. Swiatecki, T. Kodama, L. J. El-Jaick, and E. R. Hilf, Phys. Rev. C 15, 2032 (1978).

[24]A. Bohr and B. R. Mottelson, *Nuclear Structure* (Benjamin, Reading, Mass., 1975), Vol. 2, p. 513.

[25]I. Hamamoto, in *Proceedings of the International Conference on Nuclear Structure Studies Using Electron Scattering and Photoreaction, Sendai, 1972,* edited by K. Shoda and H. Ui (Suppl. Res. Rep. Lab. Nucl. Sci., Tohoku Univ., 1972). Vol. 5.

[26]J. Ahrens *et al.*, Nucl. Phys. A251, 479 (1975).

[27]C. W. Soto Vargas, D. S. Onley, and L. E. Wright, Nucl. Phys. A288, 45 (1977).

[28]W. Thomas, Naturwissenschaften 13, 627 (1923); F. Reiche and W. Thomas, Z. Phys. 34, 510 (1925); W. Kuhn, *ibid.* 33, 408 (1925).

[29]B. I. Goryachev, B. S. Ishkhanov, I. M. Kapitanov, I. M. Piskarev, V. G. Shevchenko, and O. P. Shevchenko, Yad. Fiz. 10, 252 (1969) [Sov. J. Nucl. Phys. 11, 141 (1970)].

[30]B. S. Ishkanov, I. M. Kapitanov, I. M. Piskarev, V. G. Shevchenko, and O. P. Shevchenko, Yad. Fiz. 11, 485 (1970) [Sov. J. Nucl. Phys. 11, 272 (1970)]

[31]S. Oikawa, A. Suzuki, J. Uegaki, T. Saito, H. Miyase, M. Sugawara, and K.Shoda, in *Proceedings of the International Conference on Photonuclear Reactions and Applications, Asilomar, March, 1973,* edited by B. L. Berman (Lawrence Livermore Laboratory, Livermore, 1973), p. 553.

[32]E. Wolynec, W. R. Dodge, and E. Hayward, Phys. Rev. Lett. 42, 27 (1979).

[33]Y. Tanaka, Prog. Theor. Phys. 46, 787 (1971).

[34]C. Ngo.Trong and D. J. Rowe, Phys. Lett. 36B, 553 (1971).

[35]V. M. Khvastunov, V. P. Berezovoi, V. P. Likhachev, A. A. Nemashkalo, G. A. Savitskii, and L. D. Yaroshevskii, Yad. Fiz. 25, 921 (1977) [Sov. J. Nucl. Phys. 25, 491 (1977)].

[36]B. S. Ishkanov, K. M. Kapitanov, and L. Majling, Phys. Lett. 22, 301 (1966).

[37]R. Ö. Akyüz and S. Fallieros, Phys. Rev. Lett. 27, 1016 (1971).

[38]I. S. Gulkarov, N. G. Afanasev, V. M. Khvastunov, N. G. Shevchenko, V. D. Afanasev, G. A. Savitskii, and A. A. Khomich, Yad. Fiz. 9, 478 (1968) [Sov. J. Nucl. Phys. 9, 274 (1969)].

[39]D. Drechsel, J. B. Seaborn, and W. Greiner, Phys. Rev. 162, 983 (1967).

[40]T. J. Bowles, R.J. Holt, H. E. Jackson, R. M. Laszewski, A. M. Nathan, J. R. Specht, and R. Starr, Phys. Rev. Lett. 41, 1095 (1978).

[41]I. S. Gulkarov, Yad. Fiz. 18, 519 (1973) [Sov. J. Nucl. Phys. 18, 267 (1974)]; 20, 17 (1974) [20, 9 (1975)].

[42]G. J. Wagner, Invited paper, International Conference on Nuclear Interactions, Canberra, Australia, 1978, Lecture Notes in Physics 92, 269 (1979).

[43]L. Meyer-Schützmeister *et al.*, Phys. Rev. C 17, 56 (1978).

[44]B. R. Mottelson, in *Proceedings of the International Conference on Nuclear Structure, Kingston, 1960,*

edited by D. A. Bromley and E. W. Vogt (Univ. of Toronto Press, Toronto/North-Holland, Amsterdam, 1960); A. Bohr, in *Nuclear Physics: An International Conference*, edited by R. Becker, C. Goodman, P. Stelson, and A. Zucker (Academic, New York, 1967).
[45]H. Überall, *Electron Scattering from Complex Nuclei* (Academic, New York, 1971).
[46]G. F. Bertsch and S. F. Tsai, Phys. Rep. 18C, 125 (1975).
[47]K. F. Liu and G. E. Brown, Nucl. Phys. A265, 385 (1976).
[48]S. Krewald, V. Klemt, J. Speth, and A. Faessler, Nucl. Phys. A281, 166 (1976).
[49]J. F. Ziegler and G. A. Peterson, Phys. Rev. 165, 1337 (1968).
[50]M. A. Dugay, C. K. Bockelmann, T. H. Curtis, and R. A. Eisenstein, Phys. Rev. 163, 1259 (1967).
[51]V. D. Afanasev *et al.*, Yad. Fiz. 10, 33 (1969) [Sov. J. Nucl. Phys. 10, 18 (1970)].
[52]T. Torizuka *et al.*, Phys. Rev. 185, 1499 (1969).
[53]Y. Torizuka, Y. Kojima, T. Saito, K. Itoh, and A. Nakada, Res. Rep. Lab. Nucl. Sci., Tohoku Univ. 6, 165 (1973).
[54]D. C. Kocher, F. E. Bertrand, E. E. Gross, R. S. Lord, and E. Newman, Phys. Rev. Lett. 31, 1070 (1973).
[55]D. C. Kocher, F. E. Bertrand, E. E. Gross, and E. Newman, Phys. Rev. C 14, 1392 (1976).
[56]J. Arvieux, M. Buenerd, A. J. Cole, P. de Saintignon, G. Perrin, and D. J. Horen, Nucl. Phys. A247, 238 (1975).
[57]N. Marty, M. Morlet, A. Willis, V. Comparat, and R. Frascaria, Nucl. Phys. A238, 93 (1975).
[58]Y. Torizuka *et al* , in *Proceedings of the International Conference on Photonuclear Reactions and Applications, Asilomar, 1973*, edited by B. L. Berman (Lawrence Livermore Laboratory, Livermore, 1973).
[59]C. C. Chang, F. E. Bertrand, and D. C. Kocher, Phys. Rev. Lett. 34, 221 (1975).
[60]P. Strehl, Z. Phys. 234, 416 (1970).
[61]R. Pitthan, F. R. Buskirk, E. B. Dally, J. N. Dyer, and X. K. Maruyama, Phys. Rev. Lett. 33, 849 (1974); 34, 848 (1975); in *Proceedings of the International Conference on Nuclear Structure and Spectroscopy, Amsterdam, 1974*, edited by H. P. Blok and A. E. L. Dieperink (North-Holland, Amsterdam, 1974), Vol. 2, p. 306.
[62]R. Pitthan, Z. Phys. 260, 283 (1973).
[63]R. Pitthan, F. R. Buskirk, J. N. Dyer, E. E. Hunter, and G. Pozinsky, Phys. Rev. C 19, 299 (1979).
[64]T. Kodama, private communication.
[65]G. E. Brown and M. Bolsterli, Phys. Rev. Lett. 3, 472 (1959).
[66]E. C. Halbert, J. B. McGrory, G. R. Satchler, and J. Speth, Nucl. Phys. A245, 189 (1975).
[67]P. Doll *et al.*, Phys. Rev. Lett. 42, 366 (1979).